Engineering Research Journal
journal homepage: https://erj.journals.ekb.eg/

# COMPARATIVE STUDY ON THE PERFORMANCE OF TYPE A AND TYPE B MICROPILED SYSTEMS IN SANDY SOIL UNDER VERTICAL LOADS FOR OPTIMIZING BEARING CAPACITIES

Eslam Hassan[1,*], Mohamed Rabie [2], Wagdy El Banna[3], Hussein Mostafa [4]

[1] Assistant lecturer, Faculty of Engineering at Mataria branch, Helwan University, Cairo, Egypt
[2] Professor of Geotechnical Engineering, Faculty of Engineering at Mataria branch, Helwan University, Cairo, Egypt
[3] Lecturer of Geotechnical Engineering, 15th May Institute in Cairo, Egypt
[4] Lecturer, Faculty of Engineering at Mataria branch, Helwan University, Cairo, Egypt

*Corresponding author E-mail: Eslam.ahmed2020@m-eng.helwan.edu.eg

**Abstract.** Micropiles are small-diameter drilled grouted piles. The grouting technique affects the connection between the grout and the surrounding earth. According to FHWA 2005, the most popular varieties of these techniques are Types A and B. For experimental work, these methods are the most appropriate. With an emphasis on the impact of the water-to-cement (W/C) and slenderness ratios (L/D) on performance, this study compares the bearing capacity behavior of Type A and Type B micropiles in sandy soil under compression loads. Also, a mathematical model was developed to predict pile load capacity based on settlement (δ), L/D ratio, and W/C ratio, providing a practical tool for optimizing pile design. This research emphasizes the importance of geometric properties and grout composition in enhancing micropile efficiency under various loading conditions. Based on the present study on Type A, experimental results show a load capacity (Q) reaching 6082 N at settlement (δ) of 5.08 mm for L/D=14 and W/C=0.3. Type B demonstrates higher capacities, reaching up to 7848 N at a settlement of 3.8 mm under similar conditions. These findings indicate that Type A exhibits complex behavior influenced by slenderness and W/C ratios, while Type B shows a more direct relationship with settlement. The results provide valuable insights for optimizing micropile design and performance prediction.

**Keywords:** Micropile, Single pile, Pile capacity, Grout injection, Cohesionless soil.

## 1 Introduction

Worldwide, micropiles have been embraced for a number of uses. Reducing settlement and increasing bearing capacity for pre-existing foundations is one of these uses. Two situations are included in this application. The first situation is during or after the completion of construction, micropiles are utilized to fix troublesome existing foundations. Tilting, unequal settlement, and excessive overall settlement

DOI: 10.21608/erj.2025.347167.1175
Received 01 January 2025; Received in revised form 01 January 2025; Accepted 18 January 2025
Available online 01 March 2025

are among the potential issues with current foundations. These issues are generally caused by foundation soils that are highly compressible and have a low bearing capacity, as well as by uneven soil layers and/or uneven loading circumstances. The second situation is buildings that have more stories put more strain on the already-existing structures. More carrying capacity from the foundation soil and reinforced buildings might be needed to support the increased loads. Strengthening current structures is outside the purview of this article and will not be discussed in more detail. In these situations, the majority of the loads from the buildings are carried by micropiles, which also lessen the loads that are applied directly to the earth. Nevertheless, little research has been done on the load transmission processes and deformation behavior of foundations supported by micropiles, leading to a lack of understanding.

Over the past 20 years, there have been notable improvements in micropile technology. The use of individual high-capacity components that can support large loads and enter confined places has replaced the use of networks of limited-capacity micropiles. Generally speaking, micropiles fall under the category of small-diameter deep foundations, which have diameters between 150 and 300 mm. Type A, a popular building technique, entails setting grout under a gravity head without the need for additional pressure. This technique creates a link between the pile and the surrounding soil by using tidy cement grouts or sand-cement mortars. Type B denotes the removal of the temporary drill casing while neat cement grout is pressed into the hole. Usually, injection pressures fall between 0.5 and 1 MPa to prevent excessive grout takes or hydrofracturing the surrounding ground, and to, if at all possible, keep the casing sealed during withdrawal.

Group effects, or the combined interaction of many micropiles, and the interaction of micropiles with the surrounding soil matrix, have been found to have a considerable impact on the engineering behavior of micropile-reinforced soils in studies [1] and [2]. These factors make the composite system a dependable way to increase soil stability by increasing its overall resistance and shear strength. Juran et al. [3] provided a thorough state-of-the-art evaluation that included all research and contributions to the state of micropile practice today. The building of individual micropiles, the evaluation of load-bearing capacity, movement estimation models, and the influence of group and network effects have all been discussed at some length. The authors also examined methodologies for predicting movement and geotechnical design guidelines for axial and lateral load capabilities from different countries. Micropiles have been widely used for a variety of engineering applications, including strengthening an existing building that has issues due to poor site exploration prior to construction or unforeseen soil problems, controlling differential settlements, and supporting structures subjected to additional loads by underpinning existing foundations. In their works, several academics have detailed the application of micropiles in soil reinforcing, retrofitting, and underpinning projects as [4][5],[6], [7], [8], [9], [10] and [11].

## 2 Experimental Work Description

This section delineates the experimental methodology employed to investigate the enhancement in load-bearing capacity of individual Type A and Type B micropiles when subjected to vertical loads. The study incorporates a series of variables, including the grout's water-to-cement ratio (W/C) and the slenderness (pile length / pile diameter) ratio (L/D), to examine and compare the bearing capacity behavior of these two micropile types within a sandy soil environment under vertical loading conditions.

### 2.1 The Soil Container

As the zone of effect of the micropile due to loading, the soil container must be sufficiently big to ensure that the margins of the container do not impact the test findings, in accordance with theories and earlier models of axially loaded piles [12] & [13]. [12] indicates that the influence zone beneath a pile extends

approximately six times its diameter; [13] emphasizes the importance of container dimensions, suggesting a minimum horizontal distance of 3-5 pile diameters between the pile and container boundaries. To minimize boundary effects on test results, the micropile model was designed with dimensions sufficiently large. The container measured 800 mm by 800 mm in plan and 700 mm in depth as illustrated in Fig. 1.

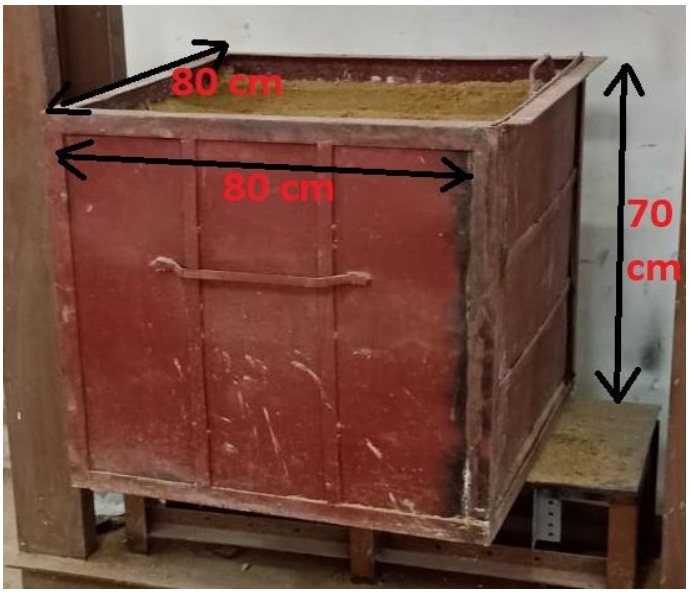


**Fig. 1.** The metal box (container) used to prepare soil samples.

## 2.2 Loading system

Using a mechanical jack system, the load was applied by placing the jack on a steel plate that was attached to the micropile head. A load cell was then mounted on the experimental frame, touching the jack's head. Settlement measurements were taken using two dial gauges. A digital screen was used to record the load, which was first started using a hand-arm gently and at an appropriate rate. For a good understanding of the experimental framework, the apparatus and experimental setup are shown in **Fig. 2.** The load was applied at a somewhat constant rate of 1 mm/min using the mechanical hydraulic jack. Additionally, the weight was transferred from the jack to the micropile via a steel plate to guarantee the pile's consistent load distribution. Additionally, the loaded steel plate and the enclosed steel plate were sufficiently attached to prevent side vibrations.

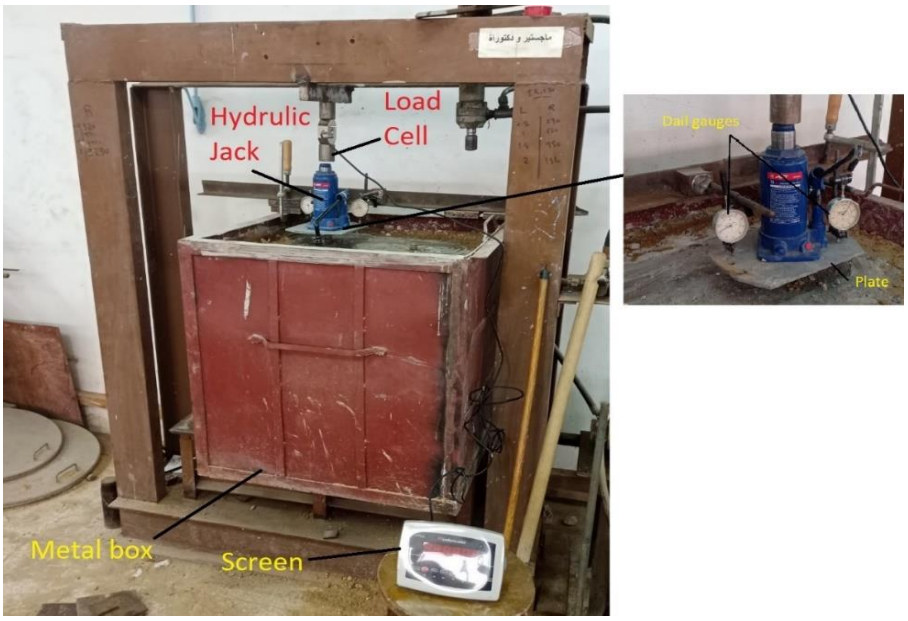


**Fig. 2**. Loading system for experimental work.

## 2.3 Micropile Model

Experimental tests of the single micropile model are performed on a hollow circular steel pipe with an outer diameter 19 mm and inner diameter 17 mm. After using bentonite liquid and a drilling instrument with the same diameter as the pipe, the outer diameter increased to 37.5 mm. Grout needs to be pumpable in addition to having a high strength and stability (bleed). Type A and Type B [14] are the types used in the present study which Type A depends on that grout is placed under a gravity head only and the cement grouts can be used, and Type B depends on using clean cement grout to fill the hole. Usually, injection pressures fall between 0.5 and 1 MPa to prevent excessive grout uptake or ground hydrofracturing. The ultimate form of the performed micropile for both kinds is shown in **Fig. 3. a & Fig. 3.b.**

**Fig. 3.a** Micropile Type A after testing

**Fig. 3.b** Micropile Type B after testing

## 2.4 Properties of Tested Soils

The current study used sandy soil, which is commonly required in compaction operations for building reasons, to examine the axial behavior and capabilities of this pile type in sand subjected to vertical loads. Changed For the sandy soil, proctor compaction tests were performed in the lab. The findings for the examined soil, including its components, classification, maximum dry density, and matching ideal moisture values, are compiled in **Table 1**. Furthermore, the angle of shearing resistance and the derived minimum dry density are shown. The compaction and particle size distribution curves for the tested soil are displayed in **Fig. 4** and **Fig. 5**.

**Table 1.** mechanical and physical characteristics of the soil under test.

| ***Parameter*** | **Maximum dry unit weight** | **Minimum dry unit weight** | **Maximum void ratio** | **Minimum void ratio** | **Specific gravity** | **Gravel** | **Coarse sand** | **Medium sand** | **Fine sand** | **Effective diameter** | **USCS Classification** | **Water content** | **Friction angle** |
|---|---|---|---|---|---|---|---|---|---|---|---|---|---|
| ***Symbol and unit*** | $\gamma_{dmax}$ ($gm/cm^3$) | $\gamma_{dmin}$ ($gm/cm^3$) | $e_{max}$ | $e_{min}$ | Gs | % | % | % | % | $D_{10}$ (mm) | SP | O.M.C (%) | Φ (degree) |
| ***Value*** | 1.93 | 1.72 | 0.52 | 0.36 | 2.62 | 13.6 | 52.9 | 33.3 | 0.21 | 0.34 | - | 5.8 | 38.3 |

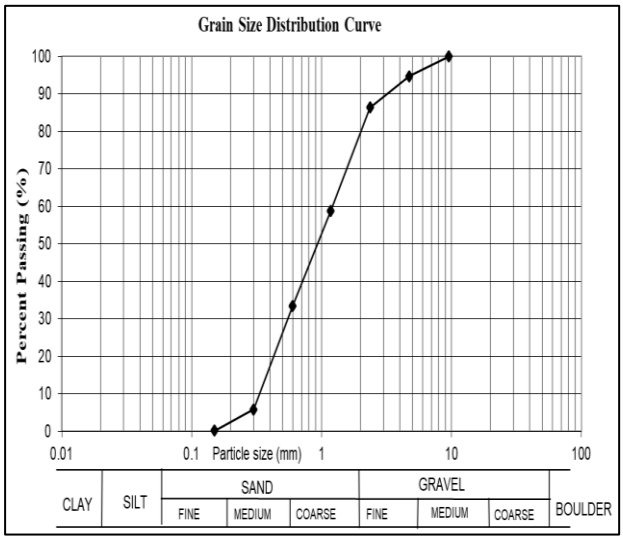


**Fig. 4.** distribution of particle sizes in the soil under test.

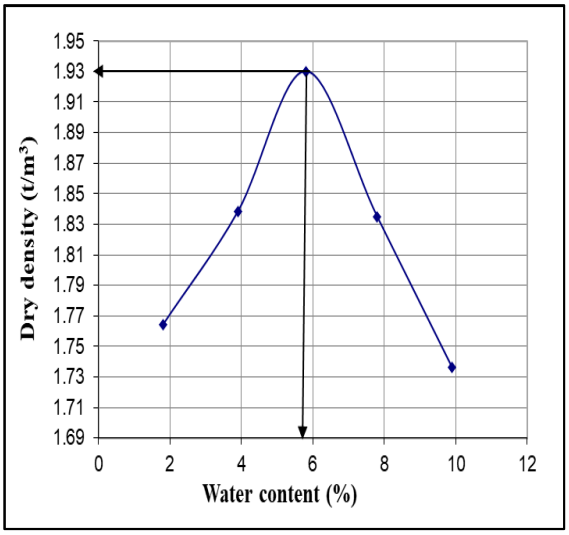


**Fig. 5.** Compaction curves using the Modified Proctor test, for the SP soil.

## 3 Experimental Work Program

To comprehend micropile behavior, an experimental work program was carried out on the previously mentioned tested soil. The purpose of the laboratory test program was to compare the bearing capacity behavior of Type A and Type B micropiles in sandy soil under vertical loads, examining the impact of various parameters as the slenderness ratio (L/D) and water–cement ratio (W/C) of grout. To evaluate the capacity of the micropile (types A & B), 18 tests were executed with changing L/D with 10, 12 &14 and W/C of grout with 0.3, 0.4 & 0.55 as shown in the laboratory test program in **Table 2.**

**Table 2.** The laboratory test program

| Test No. | L (cm) | D (cm) | L/D | Dr (%) | W/C | Type |
|---|---|---|---|---|---|---|
| 1 | 37.5 | 3.75 | 10 | 90 | 0.4 | A |
| 2 | | | | | 0.3 | |
| 3 | | | | | 0.55 | |
| 4 | 45 | | 12 | | 0.4 | |
| 5 | | | | | 0.3 | |
| 6 | | | | | 0.55 | |
| 7 | 52.5 | | 14 | | 0.4 | |
| 8 | | | | | 0.3 | |
| 9 | | | | | 0.55 | |
| 10 | 37.5 | 3.75 | 10 | 90 | 0.4 | B |
| 11 | | | | | 0.3 | |
| 12 | | | | | 0.55 | |
| 13 | 45 | | 12 | | 0.4 | |
| 14 | | | | | 0.3 | |
| 15 | | | | | 0.55 | |
| 16 | 52.5 | | 14 | | 0.4 | |
| 17 | | | | | 0.3 | |
| 18 | | | | | 0.55 | |

# 4 Testing Procedures

Phase one of the experimental testing process involved implementing the micropile, and phase two involved loading the micropile once it had been implemented. The following steps provide a summary of the first stage:

- **a)** A hole is dug to the specified depth using a specialized drilling instrument. To enable grouting with bentonite fluid, the hole's diameter is marginally greater than the micropiles. As shown in **Fig. 6.**, bentonite was injected using an appropriate drilling pump.
- **b)** As shown in **Fig. 7.**, the grout is then injected using the same pump until any last bits of dirt or bentonite liquid are eliminated from the hole.
- **c)** At this stage, putting down the micropile is done as shown in **Fig. 8.**
- **d)** This stage is the final injection for Type B in which the injection pressure fall between 0.5 and 1 MPa as shown in **Fig. 9.**
- **e)** Base plate is installed for loading preparation as shown in **Fig. 10.**

The loading of the micropile, which involved applying the load using a mechanical jack system, mounting the jack on a base plate and connecting it to the micropile head, mounting a load cell on the experimental frame and making contact with the jack's head, and measuring settlement using two dial gauges, encapsulates the second stage. The load was shown on a digital screen once the hand arm was loaded at a manageable rate. The experimental setup and instruments are described in full in **Fig. 11** to give a comprehensive understanding of the experimental context.

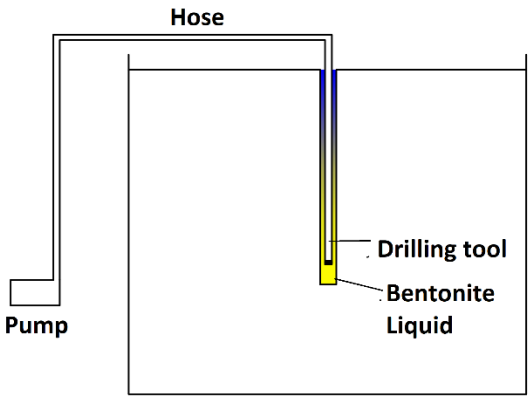


**Fig. 6.** Stage 1: Pumping Bentonite liquid

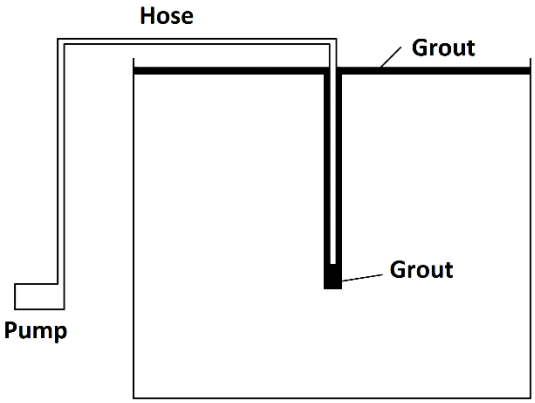


**Fig. 7.** Stage 2: Pumping Grout

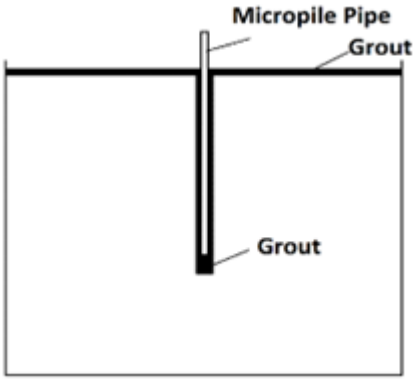


**Fig. 8.** Stage 3: Putting down the micropile

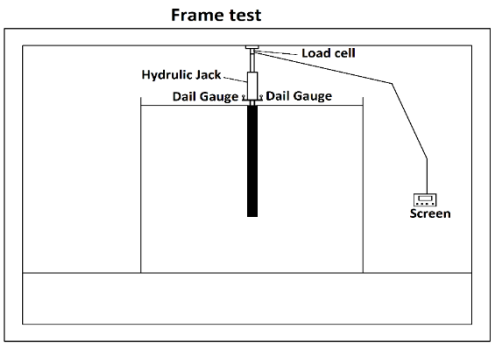


**Fig. 9.** Stage 4: Final injection for micropile (Type B)

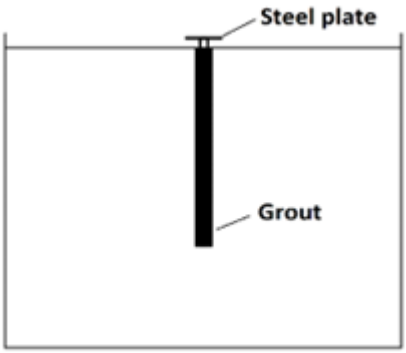


**Fig. 10.** Stage 5: Steel plate installation

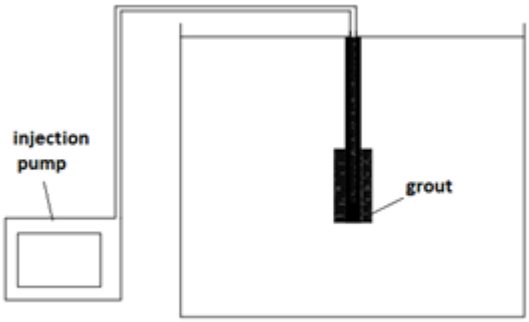


**Fig. 11.** Stage 6: Loading

## 5 Testing Results

The majority of the test program consists of compression loading studies on a single micropile model implanted in sand soil. The ultimate micropile capacity and the associated vertical displacement of failure—the point at which the displacement curve peaks or continues to climb while the micropile resistance does not increase further—were determined using the load-settlement relationship. With slenderness ratios L/D of 10, 12, and 14 and water-cement ratios W/C of 0.3, 0.4, and 0.55 for Type A and Type B, the load-displacement relationship is displayed in **Figs. 12 to 20**. The results also show that the bearing capacity of the micropiles improved significantly when the construction method was changed from Type A method to Type B method. This improvement could be attributed to better execution quality, the use of advanced tools or techniques, or enhancements in the properties of the surrounding soil during the construction process.

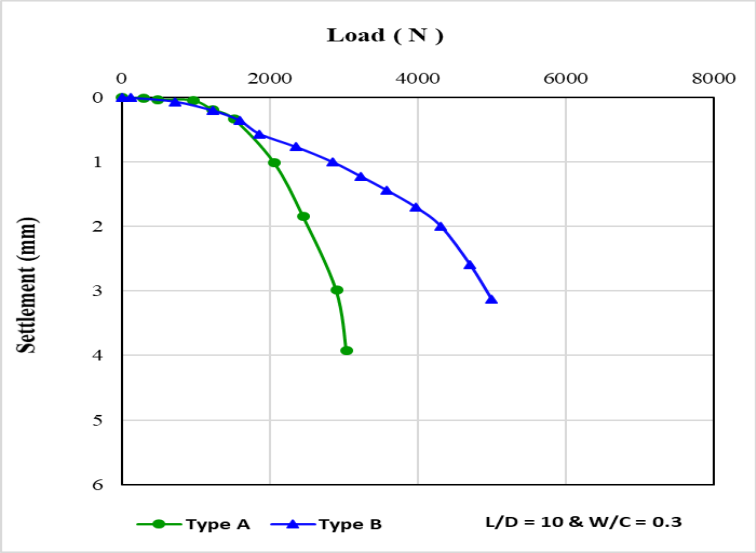


**Fig. 12.** Load-Settlement relationship for L/D = 10 at W/C = 0.3 (Types A & B)

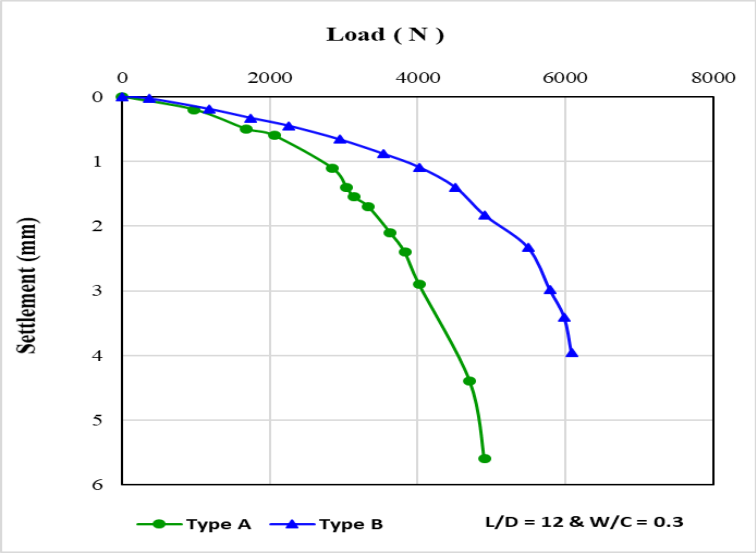


**Fig. 13.** Load-Settlement relationship for L/D = 12 at W/C = 0.3 (Types A & B)

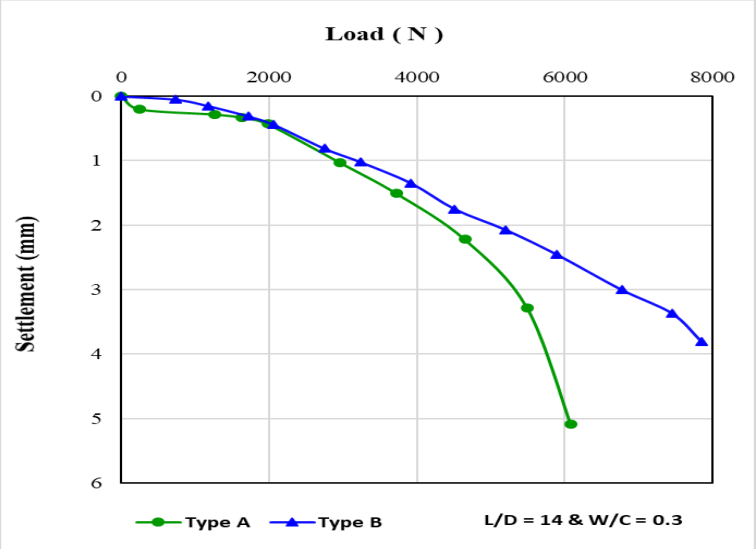


**Fig. 14.** Load-Settlement relationship for L/D = 14 at W/C = 0.3 (Types A & B)

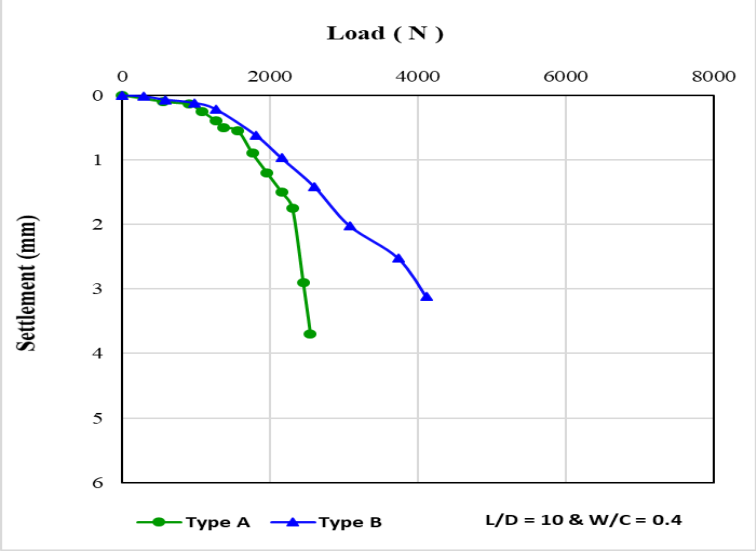

**Fig. 15.** Load-Settlement relationship for L/D = 10 at W/C = 0.4 (Types A & B)

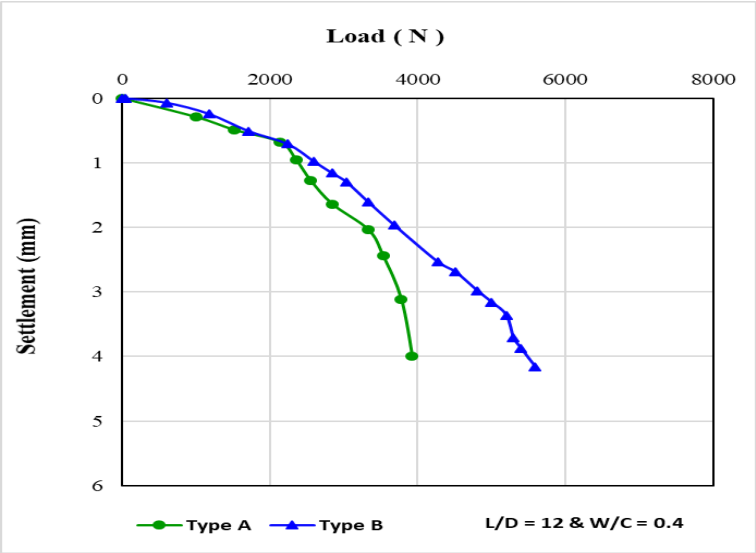


**Fig. 16.** Load-Settlement relationship for L/D = 12 at W/C = 0.4 (Types A & B)

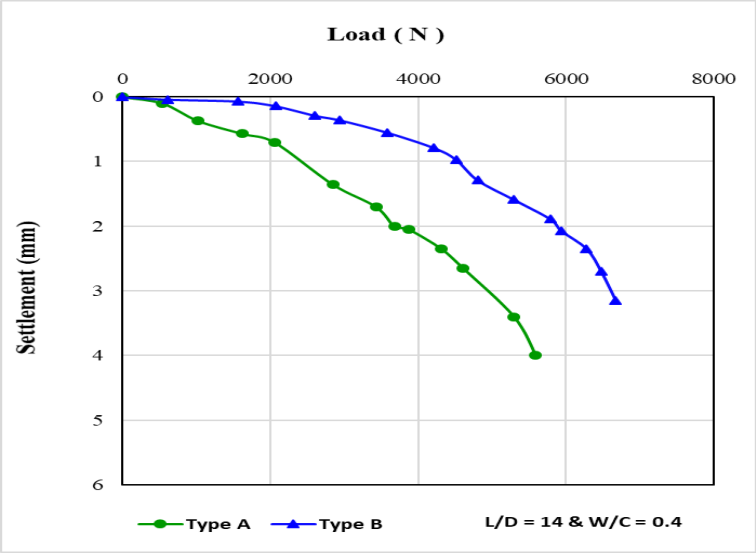


**Fig. 17.** Load-Settlement relationship for L/D = 14 at W/C = 0.4 (Types A & B)

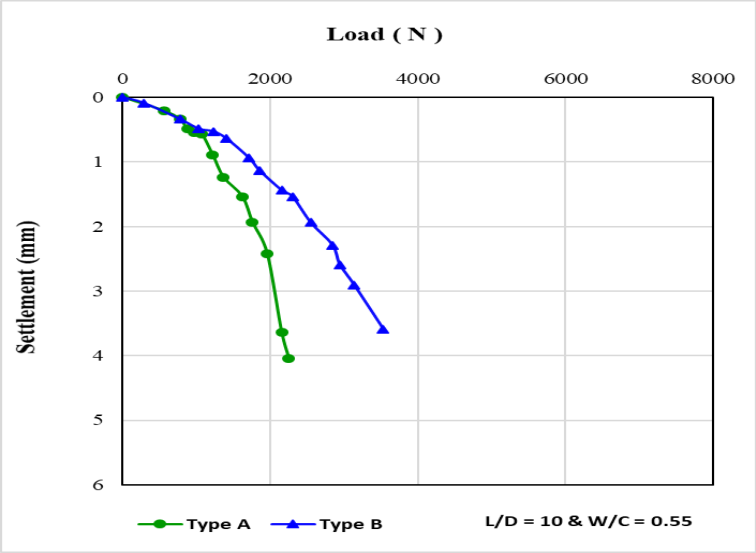


**Fig. 18.** Load-Settlement relationship for L/D = 10 at W/C = 0.55 (Types A & B)

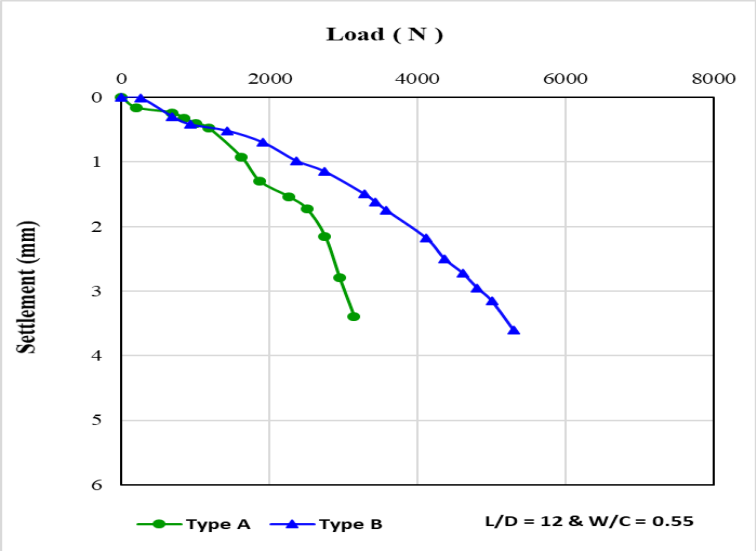


**Fig. 19**. Load-Settlement relationship for L/D = 12 at W/C = 0.55 (Types A & B)

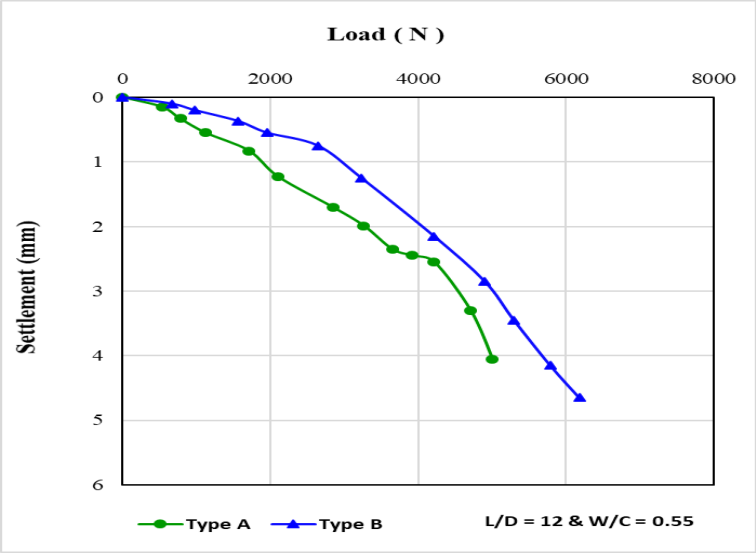


**Fig. 20.** Load-Settlement relationship for L/D = 14 at W/C = 0.55 (Types A & B)

# 6 Results analysis

## 6.1 Analysis of the results

Based on the provided graphs, we can make the following observations:

**Effect of Slenderness Ratio:**

- In general, the micropile's load-carrying ability falls as the slenderness ratio rises (from 10 to 14). This is due to the fact that thinner piles are more likely to buckle under load.
- The load-bearing capacity increases as the slenderness ratio rises, particularly at the micropile with L/D = 14, which exhibits the highest load capacity.
- The initial stiffness of the pile (slope of the curve at low loads) also tends to decrease with increasing slenderness ratio, indicating a reduction in resistance to small deformations.

**Effect of Water-Cement Ratio:**

- The micropile's ability to support loads is often reduced when the water-to-cement ratio (W/C) is increased. This is due to the fact that a greater W/C ratio results in injected grout that is weaker and less resilient to compressive pressures

**Comparison between Type A and Type B**

- Both Type A and Type B micropiles demonstrate similar load-settlement behavior, influenced by slenderness ratio (L/D) and water-to-cement ratio (W/C). However, Type A piles generally show higher stiffness and lower settlement, while Type B piles exhibit slightly higher ultimate load capacities, particularly at higher L/D ratios. The differences may arise from material properties, installation methods, or design specifications. Further investigation through regression analysis or field verification can confirm these findings.

**Overall Trend:**

- The maximum settlement is ranging from approximately 0 to 4 mm.
- The load-settlement curves exhibit a typical nonlinear behavior, with the initial portion being relatively stiff and the latter portion showing a more gradual increase in settlement with increasing load.
- The ultimate load or failure load of the pile is sometimes defined as the point on the curve when a noticeable increase in settling begins to occur.

A load equal to 10% of the micropile diameter, or settlement, is a standard way to define the micropile's ultimate load capacity. A micropile makes it challenging to calculate the settlement level for the final load capacity due to its tiny size and usage as a foundation underpinning for pre-existing foundations. [16]and [17] used the Davission's criterion [18] to define the ultimate load carrying capacity of micropiles, which would produce a conservative load-carrying capacity. [19] and [20] used the intersection method to find a load that intersects the initial and final tangent lines on load-settlement curve. **Table 3** shows the ultimate capacity of micropile and capacity at 10% of micropile diameter for Type A and Type B.

**Table 3.** The experimental test results

| Test No. | L/D | W/C | Type | Ultimate Capacity (N) | Ultimate capacity at 10% D – (N) |
|---|---|---|---|---|---|
| 1 | 10 | 0.4 | A | 2551 | 2374 |
| 2 | | 0.3 | | 3041 | 2972 |
| 3 | | 0.55 | | 2256 | 2207 |
| 4 | 12 | 0.4 | | 3924 | 3953 |
| 5 | | 0.3 | | 4905 | 4797 |
| 6 | | 0.55 | | 3139 | 3002 |
| 7 | 14 | 0.4 | | 5592 | 5464 |
| 8 | | 0.3 | | 6082 | 6004 |
| 9 | | 0.55 | | 5003 | 4934 |
| 10 | 10 | 0.4 | B | 4120 | 4124 |
| 11 | | 0.3 | | 5005 | 6075 |
| 12 | | 0.55 | | 3532 | 3380 |
| 13 | 12 | 0.4 | | 5592 | 5450 |
| 14 | | 0.3 | | 6082 | 6005 |
| 15 | | 0.55 | | 5297 | 5400 |
| 16 | 14 | 0.4 | | 6670 | 7400 |
| 17 | | 0.3 | | 7848 | 7422 |
| 18 | | 0.55 | | 6180 | 5270 |

### 6.2 Derivation of a mathematical model

A number of variables, including the pile's slenderness ratio (L/D) and the concrete's water–cement ratio (W/C), affect how micropiles behave under stress. Optimizing pile design requires an understanding of how these factors relate to the resultant load (Q) and vertical displacement (δ). The objective of this work is to use theoretical and experimental data to create an empirical equation that links these factors. Tests of pile load on micropiles with different ratios of slenderness and water-to-cement were used to get experimental results. The applied load and associated vertical displacement were measured in these experiments. The link between these variables was expressed by an equation that was developed by regression analysis and numerical modeling with **Colab Google**.

The results showed that there was a non-linear relationship between the load (Q), displacement (δ), W/C ratio, and L/D ratio. For Type B, the equation was constructed in the general form shown below:

For Type B

$$\mathbf{Q = -191.49 + 265.22\,\delta - 34.44\,\delta^2 + 33.44\,\delta\left(\frac{L}{D}\right) - 377.34\left(\frac{W}{C}\right)}$$

Where ;
Q : The load on pile – N .
δ : Vertical displacement of pile – mm .
L/D : The slenderness ratio of micropile.
W/C : The ratio of water weight to cement weight.

**Analysis of the Equations:**

**For Type B**

- The base constant −191.49 is lower than in Type A, suggesting this pile type has inherently less capacity unless enhanced by other factors
- 265.22δ: Strong positive effect of settlement, meaning load increases rapidly with small settlements.
- −377.34(W/C): Negative contribution of W/C, consistent with Type A, showing weaker grout reduces load.
- $-34.44\delta^2$: Reduction in load at higher settlements, but less steep than in Type A, suggesting Type B is less sensitive to excessive settlement.
- 33.44d(L/D): Positive interaction between d and L/D, showing slender piles gain load capacity even as settlement increases.

**Figs. 21 to 29** show verification of the derived equation with the results of experimental work for Type B.

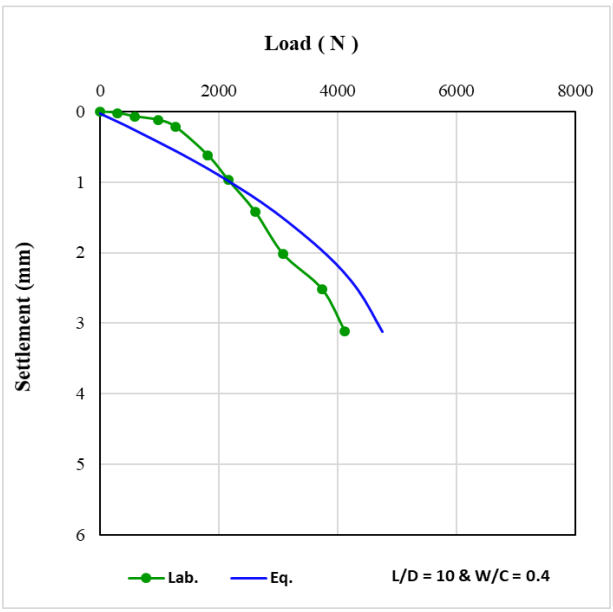


**Fig. 21.** Comparison between Derived equation & Experimental results – Test 10

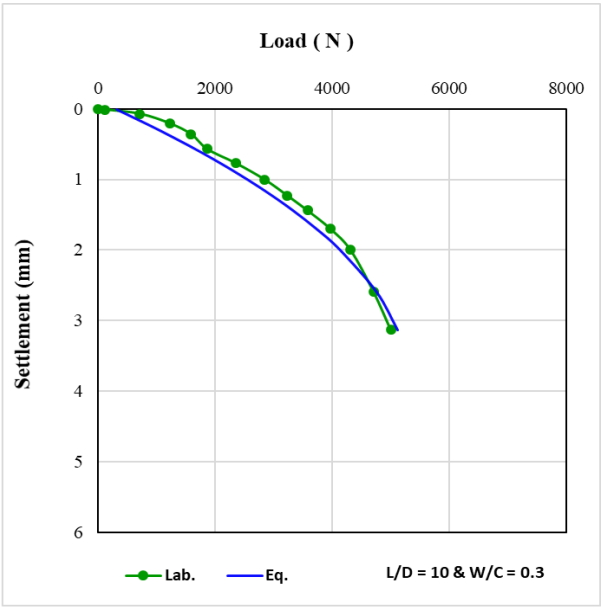


**Fig. 22.** Comparison between Derived equation & Experimental results – Test 11

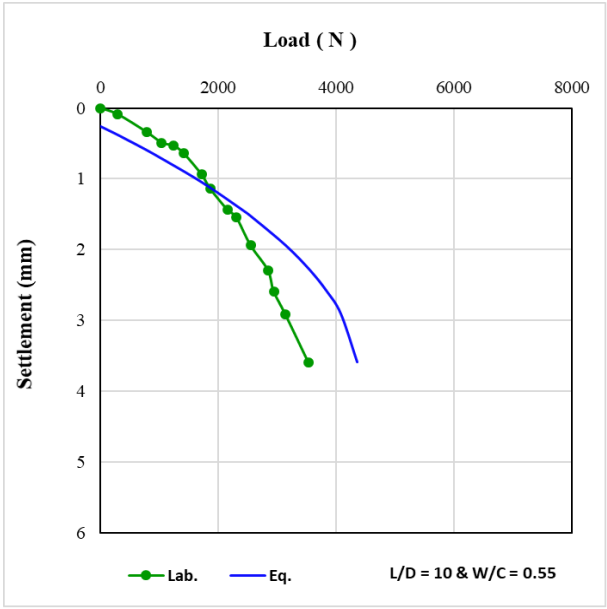


**Fig. 23.** Comparison between Derived equation & Experimental results – Test 12

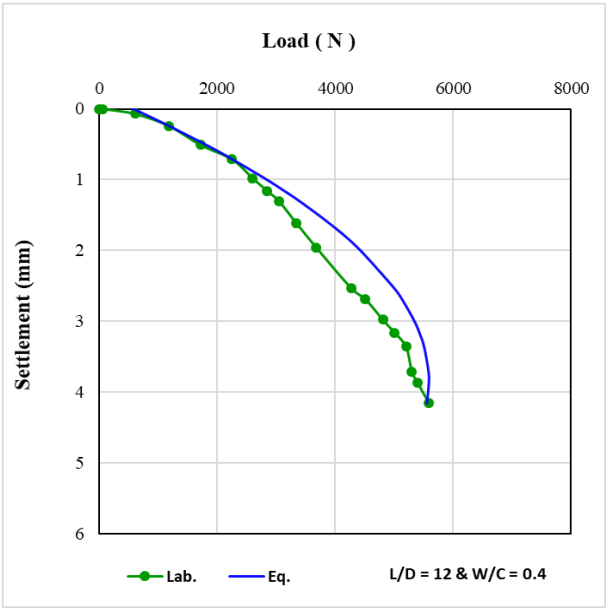


**Fig. 24.** Comparison between Derived equation & Experimental results – Test 13

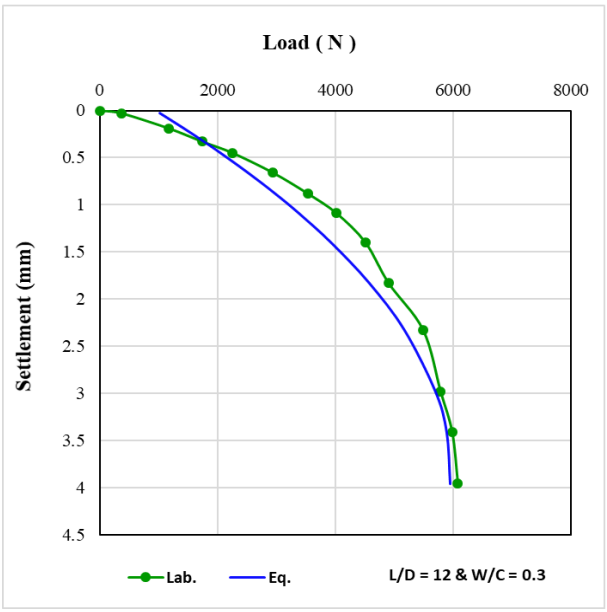


**Fig. 25.** Comparison between Derived equation & Experimental results – Test 14

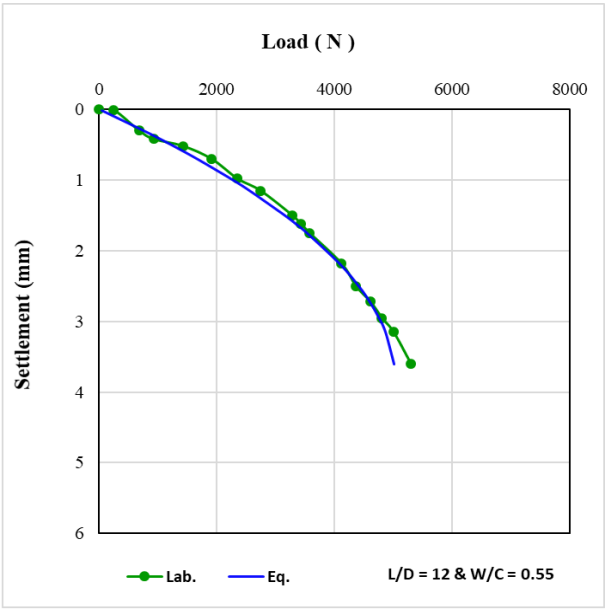


**Fig. 26.** Comparison between Derived equation & Experimental results – Test 15

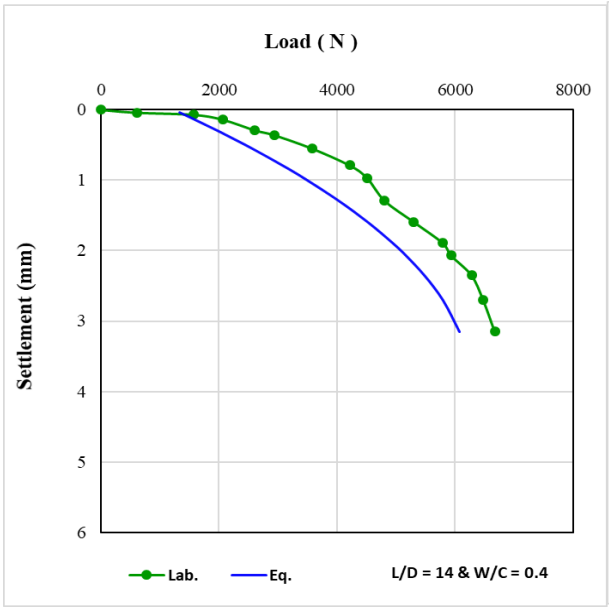


**Fig. 27.** Comparison between derived equation & Experimental results – Test 16

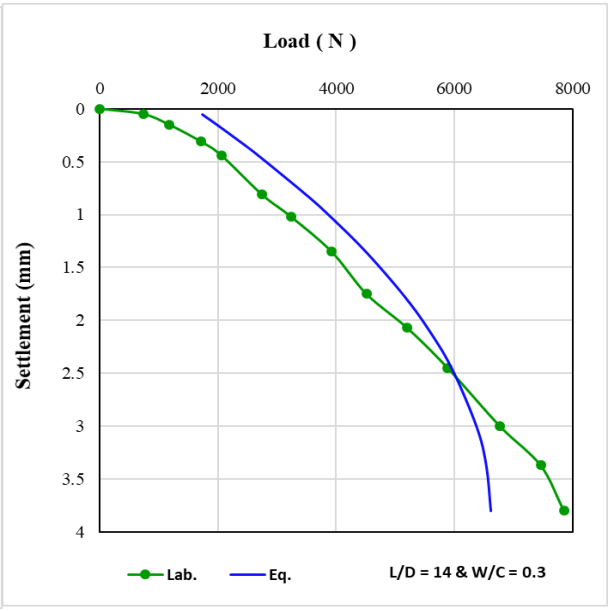


**Fig. 28.** Comparison between derived equation & Experimental results – Test 17

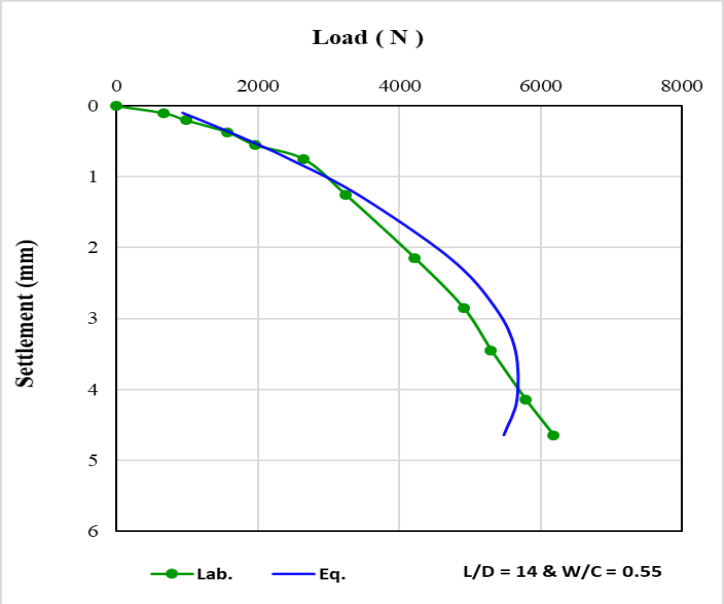


**Fig. 29.** Comparison between Derived equation & Experimental results – Test 18

# 7 Conclusions

### 1. Micropile Capacity:

- Type B consistently showed higher bearing capacity compared to Type A, with capacity increases reaching 35-45% at L/D = 14, while Type A demonstrated smaller increases in capacity.

### 2. Load-Displacement Behavior:

- Type A exhibited steeper load-displacement curves with higher stiffness but more brittle failure mechanisms. In contrast, Type B showed a more gradual load-displacement response with better displacement control and more ductile failure, making it more suitable for displacement-sensitive applications.

### 3. Water-Cement Ratio (W/C) Impact:

- Type A was more sensitive to variations in the W/C ratio, with a 30-40% reduction in strength when W/C increased from 0.3 to 0.55
- Type B showed less sensitivity, with only a 20-25% strength reduction, indicating better adaptability to field conditions.

### 4. Soil Interaction Mechanisms:

- Type B achieved better grout penetration into the surrounding soil, leading to superior skin friction and load transfer. This resulted in a higher bearing capacity, but required higher material consumption and stricter quality control.
- Type A had more controlled grout penetration and lower material usage, offering more predictable behavior, especially in layered or variable soil conditions.

5. **Cost-Effectiveness:**

- Type A involved lower material usage and installation costs, making it more economical for applications in dense or stiff soils where its superior skin friction and load transfer capacity can be fully utilized.A.
- Type B, on the other hand, required additional grout injection, leading to higher material costs and more stringent installation procedures. However, it proved more cost-effective for moderate-load applications, especially where displacement control and more gradual failure are prioritized.

6. **Long-Term Performance and Durability:**

- Type A showed superior creep resistance and long-term stability, especially under higher loads.
- Type B demonstrated more consistent long-term behavior across various loading conditions, making it suitable for projects with long-term performance and serviceability requirements.

7. **Practical Applications:**

- Type B is ideal for critical structures requiring high capacity and minimal long-term settlement, especially in dense or stiff soils where its superior skin friction can be fully utilized.
- Type A is best suited for regular structures with moderate load requirements, offering better displacement control and reliable performance.

8. **Optimal Method Selection:**

- The choice of installation method should be based on project-specific requirements, soil conditions, and economic constraints to ensure efficient and reliable micropile installations. Type A is more suited for projects prioritizing displacement control and cost-effectiveness, while Type B is best for high-load applications with less emphasis on displacement control.

9. **Derived mathematical model:**

Based on the physical characteristics and grout composition of micropiles, the obtained relationship offers a thorough tool for estimating their load capability. Type B model provides a more realistic depiction of pile behavior under various circumstances by include both linear and nonlinear factors, along with interaction effects between displacement, slenderness ratio, and water-cement ratio. This formula may be used by engineers to optimize pile design, making sure that piles are both economical and able to sustain the necessary loads.

$$\mathbf{Q} = -191.49 + 265.22\,\delta - 34.44\,\delta^2 + 33.44\,\delta\left(\frac{\mathbf{L}}{\mathbf{D}}\right) - 377.34\left(\frac{\mathbf{W}}{\mathbf{C}}\right)$$

## References

[1] F. Lizzi, 'The pali radice (root piles)" symposium on soil and rock improvement techniques including geotextiles reinforced earth and modem piling Methods Bangkok D3', 1982.

[2] C. Plumelle, 'Improvement of the bearing capacity of soil by inserts of group and reticulated micro piles', in *Proceedings*, 1984, pp. 83–89.

[3] I. Juran, D. A. Bruce, A. Dimillio, and A. Benslimane, 'Micropiles: the state of practice. Part II: design of single micropiles and groups and networks of micropiles', *https://doi.org/10.1680/gi.1999.030301*, vol. 3, no. 3, pp. 89–110, Jun. 2015, doi: 10.1680/GI.1999.030301.

[4] G. Sabini and G. Sapio, 'Behaviour of small diameter piles under axial load', *X ICSMFE*, vol. 2, pp. 823–828, 1981.
[5] F. Schlosser and I. Juran, 'Design parameters for artificially improved soils', 1981, *Br Geotech Soc*. Accessed: Oct. 14, 2024. [Online]. Available: https://nyuscholars.nyu.edu/en/publications/design-parameters-for-artificially-improved-soils
[6] F. LIZZI, 'RETICULATED ROOT PILES TO CORRECT LANDSLIDES', 1978.
[7] F. LIZZI, 'THE "RETICOLO DI PALI RADICE" (RETICULATED ROOT PILES) FOR THE IMPROVEMENT OF SOIL RESISTANCE. PHYSICAL ASPECTS AND DESIGN APPROACHES', 1983.
[8] N. SOLIMAN and G. MUNFAKH, 'Foundations on drilled and grouted mini piles : A case history', pp. 363–369, 1988.
[9] M. W. O'Neil and R. F. Pierry, 'Behaviour of Mini-Grouted piles used in of the International Conference on Piling and Deep Foundations', 1989, *London*.
[10] W. H. Ting and R. Nithiaraj, 'Underpinning a Medium-Rise Building with Micropiles-A Case History', *GEOTECHNICAL ENGINEERING*, vol. 31, no. 2, pp. i–i, 2000.
[11] D. A. Bruce, 'Small-diameter cast-in-place elements for load-bearing and in situ earth reinforcement', *Ground control and improvement, PP Xanthakos, LW Abramson, and DA Bruce, eds., Wiley Interscience, New York*, 1994.
[12] H. Hirayama, 'A unified base bearing capacity formula for piles', *Soils and foundations*, vol. 28, no. 3, pp. 91–102, 1988.
[13] Shamsher. Prakash and H. D. . Sharma, 'Pile foundations in engineering practice', p. 734, 1990, Accessed: Nov. 28, 2024. [Online]. Available: https://books.google.com/books/about/Pile_Foundations_in_Engineering_Practice.html?hl=ar&id=3ePSnCRi5kUC
[14] N. H. I. FHWA, 'Micropile design and construction–reference manual. Federal Highway Administration-National Highway Institute (FHWA NHI). US Department of Transportation, McLean, Va. Publication No', FHWA NHI-05-039, 2005.
[15] B. Sharma, S. Zaheer, and Z. Hussain, 'Experimental Model for Studying the Performance of Vertical and Batter Micropiles', American Society of Civil Engineers (ASCE), Feb. 2014, pp. 4252–4264. doi: 10.1061/9780784413272.412.
[16] Y. Huang, E. L. Hajduk, D. S. Lipka, and J. C. Adams, 'Micropile Load Testing and Installation Monitoring at the CATS Vehicle Maintenance Facility', pp. 1–10, Oct. 2007, doi: 10.1061/40902(221)28.
[17] J. R. Wolosick, 'Ultimate Micropile Bond Stresses Observed during Load Testing in Clays and Sands', pp. 12–22, Mar. 2009, doi: 10.1061/41021(335)2.
[18] S. Alampalli and V. Peddibotla, 'High capacity piles', *Proc. Innovations in Found. Const.*, vol. 52, no. 2, pp. 61–69, Jun. 1972, doi: 10.3208/SANDF.37.2_61.
[19] A. J. Lutenegger, 'Low Energy Compacted Concrete Grout Micropiles', pp. 146–157, Jan. 2004, doi: 10.1061/40713(2004)6.
[20] S. Bhardwaj and S. K. Singh, 'Experimental Study on Model Micropiles under Oblique Pullout Loads', pp. 610–621, May 2014, doi: 10.1061/9780784413449.059.